Using Linear and Non Linear Stability Theory for Evaluating Code Accuracy

Marcello A. Faraco de Medeiros
USP - Universidade de São Paulo
Escola de Engenharia de São Carlos - Departamento de Engenharia Aeronáutica
Av. Trabalhador São Carlense, 400 - São Carlos, SP - 13566-590, Brazil
marcello@sc.usp.br

Jorge H. Silvestrini
Pontifícia Universidade Católica do Rio Grande do Sul
Av. Ipiranga 6681, Predio 30 - Porto Alegre, RS - 90619-900, Brazil
jorgehs@em.pucrs.br

Márcio T. Mendonça
Centro Técnico Aeroespacial, Instituto de Aeronáutica e Espaço
Pç Mal. Eduardo Gomes, 50 - São José dos Campos, SP - 12228-904, Brazil
marcio_tm@yahoo.com

Abstract. *Code accuracy is a very important aspect of both DNS and LES simulation. Verification of the accuracy of such codes is often performed by comparison with the theoretical solutions of selected linear stability problems. An example of the procedure is given in the paper. However, in many instances the linear stability analysis becomes a very complicated task, in particular when viscous and compressibility effects are considered. The paper shows that an alternative approach can be provided by the nonlinear stability analysis. The nonlinear stability tests can be simpler than the linear ones because the details of the analysis are no necessary. The nonlinear stability tests may not substitute the linear ones in all aspects, but are equally demanding and permit an estimation of the numerical error of the code. An application of the method is given for the a free-shear layer flow, but it can be extended for boundary layers if three-dimensionality is included.*

Key words: *Direct numerical simulation, hydrodynamic stability, compact difference schemes, high order methods, shear layer, Kelvin-Helmholtz instability*

1. Introduction

In direct Navier-Stokes or Large Eddy Simulations, code accuracy becomes really an issue. In the former, one wants to simulate all the scales of turbulence, and if the numerical error is large the fine details of the small scale turbulence are lost. In the latter, accuracy is just as important. There, the numerical error can act as a non-physical sub-grid turbulence model and can affect the results. Code testing is therefore of paramount importance in this field.

Almost always the accuracy that is expected from these simulations is higher than the experimental accuracy of the most carefully done experiment. To check the accuracy one has to rely on analytical solutions of the Navier-Stokes equations for comparison. There are very few such solutions and even less if the solution is to vary in two or three-dimensions and in time. Often linear stability theory comes in hand. Both the eigenfunctions and the eigenvalues of the linear stability analysis can be used for code testing, as explained in the sections bellow. In fact, the solutions of the linear stability problems are seldom analytical. However, they can be cast into a two point boundary condition problem in one dimension and therefore can easily be solved numerically with very high accuracy in an extremely fine computational grid at low cost. For the purpose of testing Navier-Stokes solvers they can be considered analytical.

However, in many circumstances the linear stability analysis becomes an issue in itself. The analysis is sometimes quite involving and perhaps other simpler tests can be helpful. The current paper presents some tests based on the nonlinear stability theory that might be of interest to researchers in the field. The tests are related to the temporal instability of a parallel free-shear flow.

2. Linear stability analysis

Linear stability analysis is a well established procedure. Details of such kind of analysis can be found in (Betchov and Criminale, 1967) and (Mendonça, 2000). The analysis for the free-shear layer is given here to make the paper more self-contained.

In the usual notation, the equations of motion for an incompressible flow in two dimensions with both viscosity and body forces neglected read

$$\frac{\partial u}{\partial x} + \frac{\partial v}{\partial y} = 0 \tag{1}$$

$$\frac{\partial u}{\partial t} + u\frac{\partial u}{\partial x} + v\frac{\partial u}{\partial y} + \frac{1}{\rho}\frac{\partial p}{\partial x} = 0 \tag{2}$$

$$\frac{\partial v}{\partial t} + u\frac{\partial v}{\partial x} + v\frac{\partial v}{\partial y} + \frac{1}{\rho}\frac{\partial p}{\partial y} = 0. \tag{3}$$

For a linear stability analysis the flow is decomposed into a base flow ($\mathbf{V}$), which is steady, and a perturbation ($\mathbf{v}^{'}$), which is considered small. If the base flow is assumed parallel, one has:

$$\mathbf{V} = (U(y), 0, 0). \tag{4}$$

Therefore, the flow field can be written as:

$$\begin{aligned} u &= U(y) + u^{'}(x,y,t) \\ v &= v^{'}(x,y,t) \\ p &= p^{'}(x,y,t). \end{aligned} \tag{5}$$

Substituting into the equations 1 to 3 and neglecting nonlinear terms yields

$$\frac{\partial u^{'}}{\partial x} + \frac{\partial v^{'}}{\partial y} = 0 \tag{6}$$

$$\frac{\partial u^{'}}{\partial t} + U\frac{\partial u^{'}}{\partial x} + v^{'}\frac{\partial U}{\partial y} + \frac{1}{\rho}\frac{\partial p^{'}}{\partial x} = 0 \tag{7}$$

$$\frac{\partial v^{'}}{\partial t} + U\frac{\partial v}{\partial x} + \frac{1}{\rho}\frac{\partial p^{'}}{\partial y} = 0. \tag{8}$$

The coefficients do not have an explicit dependency on t and x. Therefore a Fourier transformation can be applied in the x direction and a Laplace transformation in time. The variables can then be written in the form:

$$\begin{aligned} u^{'}(x,y,t) &= \frac{1}{2}\left[\hat{u}(y)e^{i(\alpha x - \omega t)}\right] + cc \\ v^{'}(x,y,t) &= \frac{1}{2}\left[\hat{v}(y)e^{i(\alpha x - \omega t)}\right] + cc \\ p^{'}(x,y,t) &= \frac{1}{2}\left[\hat{p}(y)e^{i(\alpha x - \omega t)}\right] + cc, \end{aligned} \tag{9}$$

where cc denotes complex conjugate. Substituting into the equations 6 to 8 yields

$$i\alpha\hat{u} + \frac{\partial \hat{u}}{\partial y} = 0 \tag{10}$$

$$i\alpha(U-c)\hat{u} + \hat{v}\frac{\partial U}{\partial y} + i\alpha\hat{p} = 0 \tag{11}$$

$$i\alpha(U-c)\hat{v} + \frac{\partial \hat{p}}{\partial y} = 0, \tag{12}$$

where c is the phase velocity which is equal to ω/α. Combining equations 11 and 12 eliminates p and using equation 10 eliminates u. The result is known as the Rayleigh Equation

$$(U-c)(v^{''} - \alpha^2 v) - U^{''}v = 0. \tag{13}$$

In order to simplify the notation the hat ($\hat{}$) has been dropped and the primes, here, denote derivatives with respect to y.

The equation constitutes an eigenvalue problem. It is solved for given U and α, with the boundary conditions that v vanishes at $y \to \pm\infty$. The eigenvalue is c while the solution $v(y)$ is the eigenfunction. In a temporal analysis c is allowed to be complex. If the imaginary part of c is positive for at least one α, the flow is considered unstable.

For the free-shear layer the base flow is given by

$$U(y) = \tanh(y). \tag{14}$$

Therefore, for $y \to \pm\infty$, $U^{''} \to 0$. In these regions equation 13 can be simplified and the solutions are:

$$\begin{aligned} v(y) &= e^{-\alpha t} \text{ for } y \to \infty \\ v(y) &= e^{\alpha t} \text{ for } y \to -\infty. \end{aligned} \tag{15}$$

(16)

One can use these solutions as boundary conditions for v in the Rayleigh Equation 13 and reduce the computational domain. In the case of the hyperbolic tangent velocity profile, the domain $[-5, 5]$ is enough to produce reasonably accurate results if α is not too small. Higher accuracy can however be achieved, even for limited computational domains, with other approaches (Michalke, 1964)

In the current paper the Rayleigh Equation was solved using a shooting method. The solution is started at one end and the eigenvalue is adjusted iteratively until the boundary condition at the other end is satisfied. The integration in y was carried out by a fourth order Runge-Kutta scheme and a Newton-Raphson algorithm was used to search for the eigenvalue. Because the base flow profile is anti-symmetric with respect to the inflexion point ($y = 0$), it follows that, provided the unstable eigenfunction is unique, the real part of c, which is the phase velocity, is null (Tatsumi and Gotoh, 1960).

$$\Re(c) = c_r = U(0) = 0. \tag{17}$$

Figure 1 gives the imaginary part of c times α as a function of α. It is seen that the flow is unstable for $0 < \alpha < 1$.

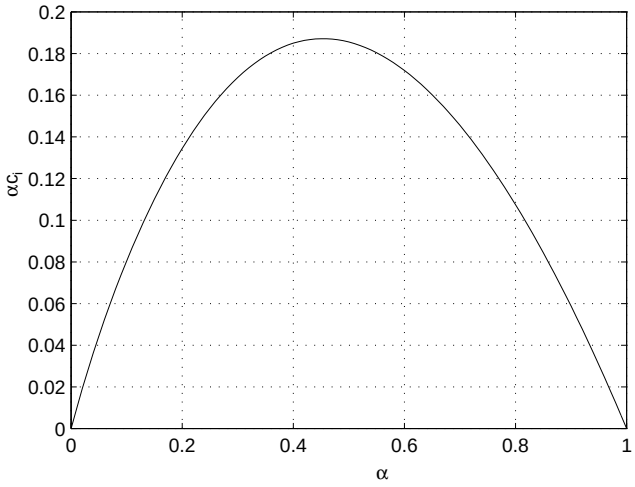

Figure 1: Growth rate αc_i as a function of α.

It is possible to evaluate the accuracy of the computational code by comparing the eigenfunctions and the growth rates extracted from the computational results with those given by the theory. However, it is important that the computational results satisfy the approximations of the linear stability theory, which is achieved by enforcing a parallel flow and by perturbing the flow with very small disturbances.

3. Nonlinear stability analysis

When the disturbances become large the linear approximations do not hold. One then needs to considered nonlinear effects. The theory associated with these effects is a little bit more complicated than their linear counterpart. It is not going to be presented here, but reviews of the subject can be found in (Herbert, 1988; Medeiros, 2000). The summary of the main results, given below, is enough for carrying out the tests proposed.

Both theory and experiment show that in the free-shear layer flow the disturbances do not grow to infinity. Instead they saturate in a limit cycle pattern of co-rotating vortices. In turn, the vortices are themselves unstable to a subharmonic disturbance. It means that if a sub-harmonic oscillation exists in the flow this oscillation will grow. The result is the pairing of vortices. It is important to emphasize that in the system there is no mechanism of production of sub-harmonic, but only amplification. There must be a , so called, seed of sub-harmonic waves for them to grow. In the numerical solutions of the equations of motion this seed may come from the numerical error that builds up during the calculations. The growth of subharmonic or otherwise provides a good indication of the numerical error of CFD codes, as shown in the next section.

4. Numerical methodology

The results to be presented here were obtained from Direct Numerical Simulation of the Navier-Stokes equations (DNS) for compressible flows (Silvestrini, 2000). The formulation used the primitive variables. For this formulations, the Navier-Stokes equations for a compressible flow are given in a cartesian coordinate system by:

$$\frac{\partial \rho}{\partial t} + \frac{\partial \rho u_j}{\partial x_j} = 0, \tag{18}$$

$$\frac{\partial \rho u_i}{\partial t} + \frac{\partial \rho u_i u_j}{\partial x_j} = -\frac{\partial p}{\partial x_i} + \frac{\partial \tau_{ij}}{\partial x_j}, \tag{19}$$

$$\frac{\partial E}{\partial t} + \frac{\partial u_j (E+p)}{\partial x_j} = -\frac{\partial q_j}{\partial x_j} + \frac{\partial u_j \tau_{ij}}{\partial x_j}, \tag{20}$$

where u_i are the components of the velocity vector in the reference frame x_i, ρ is the density, p is the pressure and $\tau_{i,j}$ is the viscous stress tensor. This tensor is written as

$$\tau_{ij} = \mu \left(\frac{\partial u_j}{\partial x_i} + \frac{\partial u_i}{\partial x_j} - \frac{2}{3} \frac{\partial u_k}{\partial x_k} \delta_{ij} \right), \tag{21}$$

where μ is the dynamic viscosity. The total energy per unit volume E is given by the relation:

$$E = \frac{p}{\gamma - 1} + \frac{1}{2} \rho u_i u_i, \tag{22}$$

where $\gamma = c_p / c_v$ is the specific heat ratio. The heat flux is evaluated by the Fourier law:

$$q_j = \lambda \frac{\partial T}{\partial x_j}, \tag{23}$$

where λ is the thermal conductivity and T, the temperature. In addition, p, ρ and T satisfy the ideal gas law:

$$p = c_p \frac{\gamma}{\gamma - 1} \rho \, T. \tag{24}$$

The equations were solved with a finite-difference scheme. The time integration was performed by a fourth order Runge-Kutta scheme (Williamson, 1980). For the calculation of the spacial derivatives a sixth order compact formulation was used (Lele, 1992). Details of the numerical scheme can be found in (Fortuné, 2000).

5. Computational tests

5.1. Linear stability

The evolution of a small sinusoidal disturbance in a free shear layer of the hyperbolic tangent type was simulated. A relatively high Reynolds number was chosen to ensure that the viscous effects were small. Also, a small Mach number was used to keep the compressibility effects negligible. In the simulation the boundary condition in the y direction was free-slip. Ideally, one would like enforce a vanishing perturbation velocity at a very large distance from the shear layer, but that requires very large computational domain. Another possibility is to use an exponential decay,except that it is only rigorously correct in the linear regime. For a sufficient large distance from the shear layer, however, the free-slip boundary condition should produce accurate results. In the horizontal direction periodicity was enforced.

Another important aspect to the considered is the treatment of the vertical diffusion. This diffusion increases the width of the shear layer during the simulation, which implies a variation in time of the base flow. Therefore, there will be a corresponding variation of the amplification rate, even in the linear regime. This would blur the picture and make it difficult to intrepret the results. The strategy adopted here was to cancel the vertical diffusion terms. This however, may have yielded an effectively inviscid formulation, since the vertical diffusion dominates over the horizontal one. This issue is further discussed below.

The wavenumber α of the disturbance selected for the simulation was $\pi/8 \approx 0.39$. This is close to the wavenumber of maximum amplification. The initial amplitude of the perturbation was approximately 10^{-6}. In figure 2 the dotted line gives the time evolution of the amplitude, obtained from the simulation. The vertical coordinate is in logarithm scale. Clearly there is a region of exponential amplification which corresponds to the regime governed by the linear theory. The theoretical result obtained with the Rayleigh Equation 13 is given by the dashed line. It overestimates the amplification rate. The disagreement could be attributed to numerical error, but they might also have come from compressibility or viscous effects. Indeed, the simulation could not be carried out at Mach number below 0.4, because of convergence problems related to the simulation of incompressible flows with a compressible formulation. Other researchers (Sandham and Reynolds, 1991) have show that there are important compreesible effects at this Mach number. The Reynolds number for the simulations was 500, which again may not have been enough for the viscous effects to be negligible. It is possible to develop a linear stability theory that includes both viscous and compressibility effects (Sandham and Reynolds, 1991) however, this is a much more difficult analysis. For a Mach number equals to 0.4 and a Reynolds number equals 500 reference (Sandham and Reynolds, 1991) gives an amplification rate of about 0.28. This is represented by the dashed-dotted line in figure 2. Now the amplification is underestimated. However, it should be recalled that, in order to reproduce a steady base flow, the vertical diffusion had to be prevented

in the simulations. Therefore, for comparison it may be more appropriate to consider an inviscid flow. Indeed, from reference (Sandham and Reynolds, 1991) the amplification rate for an inviscid flow at Mach number 0.4 is approximately 0.3. In figure 2 this corresponds to the solid line. The agreement is remarkable, but with so many adjustments the test may be considered not entirely conclusive.

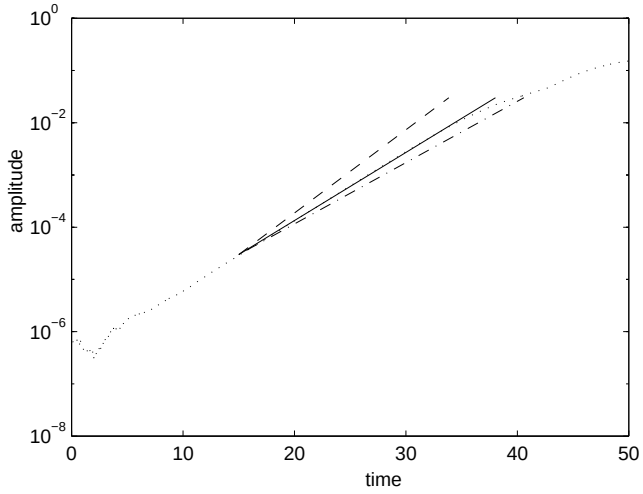

Figure 2: Amplitude evolution. Dotted line is the computational result. Dashed line represents the prediction from an inviscid incompressible theory. The dashed-dotted line is the prediction from a viscous compressible analysis. The solid line is the inviscid compressible prediction.

The eigenfunction was also extracted from the simulation results. In figure 3, it is compared with that from an inviscid incompressible theory. In the theoretical solution presented in figure 3 the computational domain was $[-15, 15]$. There are differences that may again be attributed to compressibility or viscous effects. They may also have come from the boundary condition in the y direction.

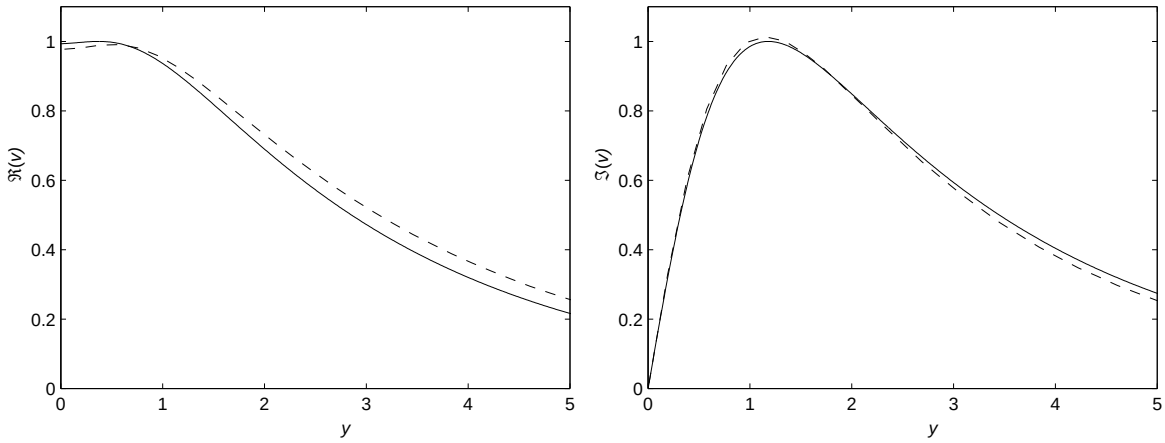

Figure 3: The normalized real (a) and imaginary (b) parts of the eigenfunctions. The dashed line is the numerical results, while the solid is line the prediction from an inviscid incompressible analysis.

5.2. Nonlinear stability

The use of nonlinear theory may constitute a way around the difficulties associated with the linear theory. Some examples are here presented to illustrate the use of nonlinear theory for code testing. In these simulations the vertical diffusion was included.

Figure 4 shows the sequence of events that usually takes place in the two-dimensional nonlinear evolution of disturbances in a free-shear layer, as discussed in the section 3. The results were obtained from simulations, but are consistent with experimental observations. The boundary conditions were identical to those used for the linear tests. The excitation was a mode of wavenumber $\pi/8$ with an additional small white noise. The amplitude of the dominant mode was 10^{-3}, while the amplitude of the white noise was 10−4. Initially, in the linear regime, the disturbance is very small and displays a sinusoidal pattern. Later two vortices are formed,

which corresponds to the limit cycle oscillation. The vortices dissipate due to viscous effects. Finally a pairing occurs between the two vortices and one large vortex results. This corresponds to the growth of the subharmonic seed.

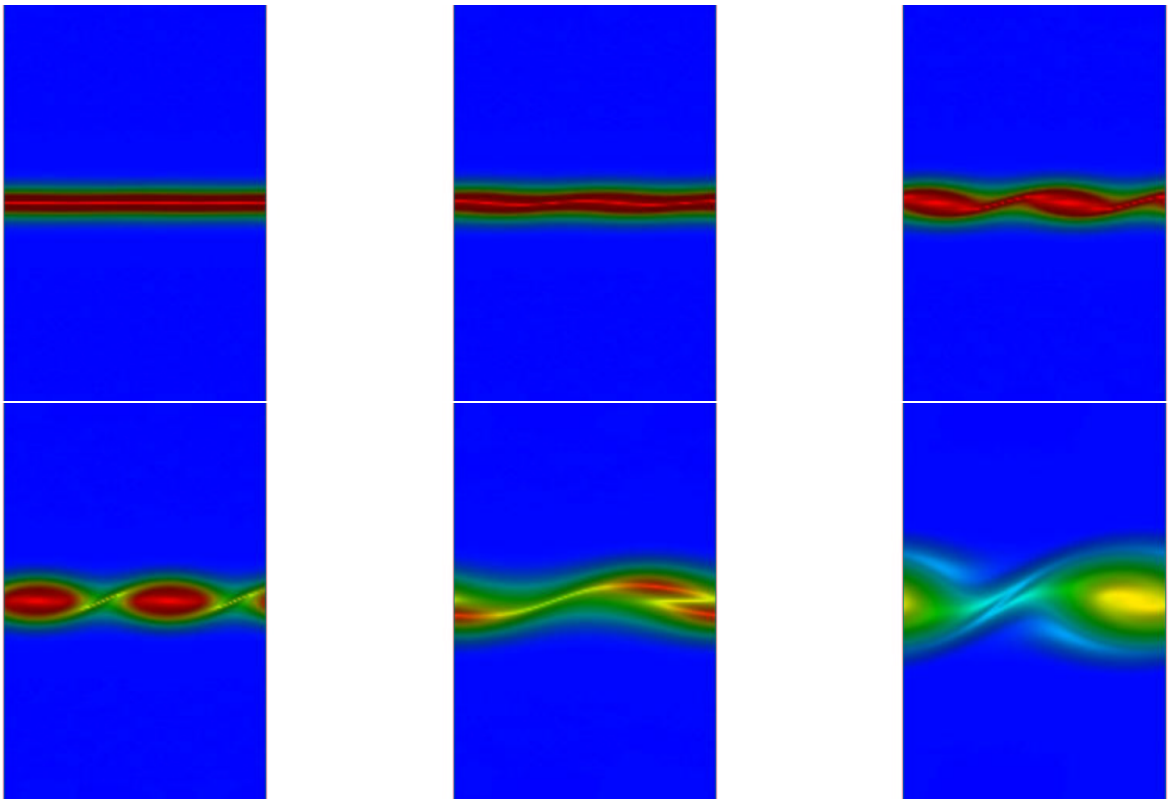

Figure 4: The linear and nonlinear evolution of disturbance composed of a dominant mode and a white noise in a shear layer. The frames presented correspond to the nondimensional times 4.48, 10.88, 17.28, 23.68, 55.68 and 89.6.

As a reference for the nonlinear tests, first a simulation was carried out with an excitation composed of a disturbance with wavenumber $\pi/8$ and a small subharmonic disturbance. The amplitude of the fundamental mode was identical to that of the previous simulation and the amplitude of the subharmonic was identical to that of the white noise. The subharmonic content was, therefore, higher than that in the white noise. Accordingly the pairing should develop more quickly, which is confirmed by figure 5.

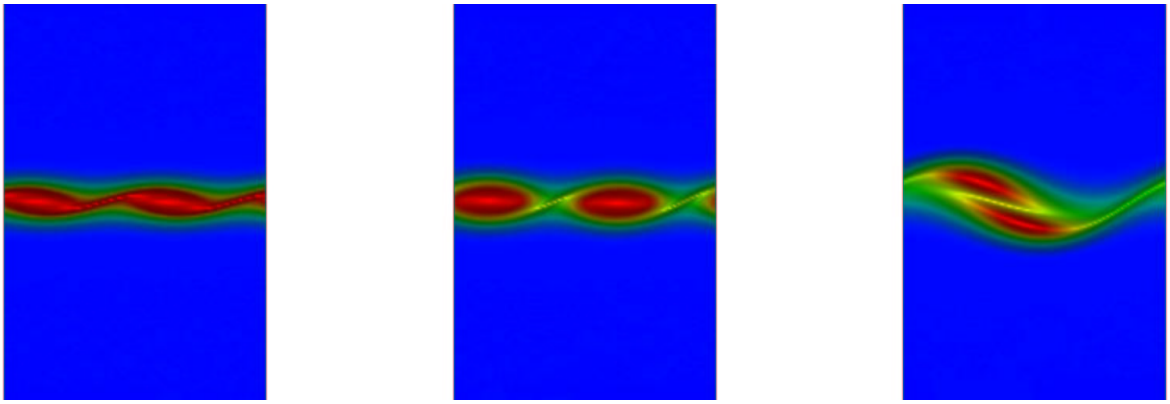

Figure 5: The linear and nonlinear evolution of disturbance composed of a dominant mode and a subharmonic seed. The frames presented correspond to the nondimensional times 17.28, 23.68, and 36.48.

Next only one wave mode, namely, that with wavenumber $\pi/8$, was excited. Under these circumstances the nonlinear theory predicts no pairing. The amplitude of the mode was slightly higher than that of the simulations above. Figure 6 shows that indeed the vortices take a rather long time to pair. It occurred only when the vortices were almost entirely dissipated by viscous effects. Since the subharmonic excitation was not

excited, the necessary subharmonic seed for the pairing must have arisen from the numerical error. Neverthless it is clear that the numerical error was much smaller than the amplitude of the subharmonic disturbance introduced. An estimate of the numerical error could be obtained if a series of tests were carried out with decreasing subharmonic disturbance amplitude until the results become similar to that of the case without the subharmonic disturbance.

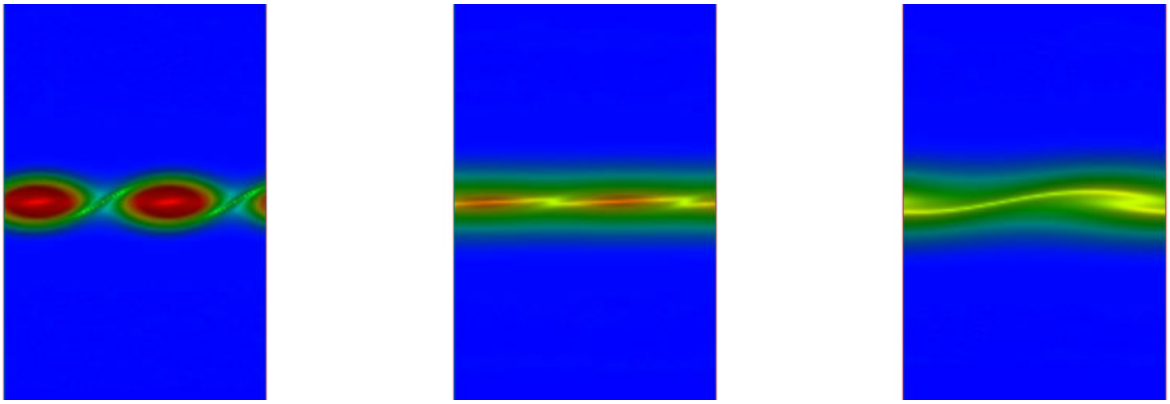

Figure 6: The linear and nonlinear evolution of disturbance composed of only one mode. The frames presented correspond to the nondimensional times 23.68, 89.6 and 112.

Although apparently simple, these tests are quite challenging for codes of second or even fourth order accuracy in space. However, even more difficult tests can be set. In the following example two modes were excited, one with wavenumber $\pi/8$ and the other with wavenumber $\pi/12$. The wavenumbers were not multiple of each other, so the pairing that took place displayed a more complicated pattern. For this simulations, the computational domain was increased in the horizontal direction by a factor three. Initially six vortices were formed. They did not have identical amplitudes, but were modulated. This derives from the fact that two different modes were excited. At some stage the neighboring smaller vortices came close together. Eventually a pairing took place and four vortices resulted. This is linked to the increase of the mode with wavenumber $\pi/12$.

The simulation proceeded with four vortices of two different amplitudes. The larger ones arose from the pairing. Apparently the picture is perfectly symmetrical indicating that the system was in equilibrium. There was no tendency of pairing because the sub-harmonic wavenumber of this distribution was not excited. But at very late times a pairing occurs. Again, this subharmonic mode must have been seeded by the numerical error, which was very small compared to the amplitude of the perturbations introduced. Clearly, the dramatic events associated with the first pairing were very accurately resolved, since the subharmonic content of numerical error was kept low. Again, in this example a series of tests with a subharmonic seed could be carried out in order to estimate the magnitude of the numerical error.

It is also interesting to check whether the error is of the truncation or the round-off type. In order to do that, an identical simulation, but with double precision accuracy, was carried out. The results in figure 8 show no pairing. Instead the smaller vortices are stretched by the larger ones while keeping a symmetrical pattern. This proves that the error was of the round-off type. In other words, for this kind of problem there is little point in refining the computational grid or in increasing the order of accuracy of the algorithm. If higher accuracy is required one should start to think about the new generation of computers.

6. Final Remarks

From the discussion above it appears that the nonlinear stability analysis provides an interesting approach for verifying code accuracy. However, it should be emphasized that this verification does not substitute that related to the linear stability theory. For instance, linear stability of flat plate boundary layer flow constitute a very demanding test for wall boundary conditions (von Terzi et al., 2001). In fact, the different analysis permit insight into different aspects of the accuracy of a code.

One important consideration is that the nonlinear tests suggested here do not require a precise solution of the nonlinear stability problem. That is not the case for the linear stability tests which do require the details of the analysis of the test flow. Since the linear stability analysis is often a very complicated issue, the nonlinear tests can be simpler to perform. The nonlinear stability theory tests are very demanding. Also, they can provide an estimate of the numerical error by comparing the solution with and without the introduction of disturbances that trigger the nonlinear stability. The procedure can easily be extended for boundary layer, if three-dimensionality in taken into account.

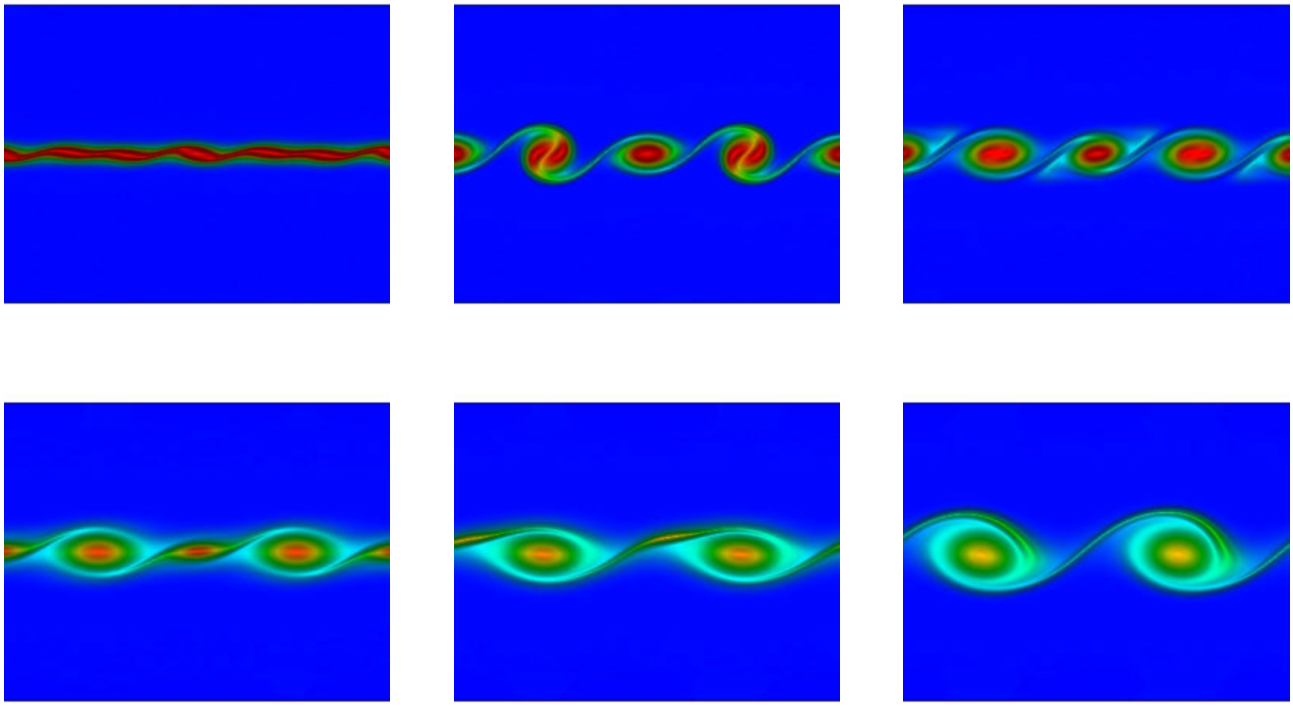

Figure 7: Nonlinear evolution of disturbance composed of a mode with wavenumber $\pi/8$ and another with wavenumber $3\pi/16$. The frames presented correspond to the nondimensional times 12.8, 25.6, 44.8, 96, 115.2 and 124.8.

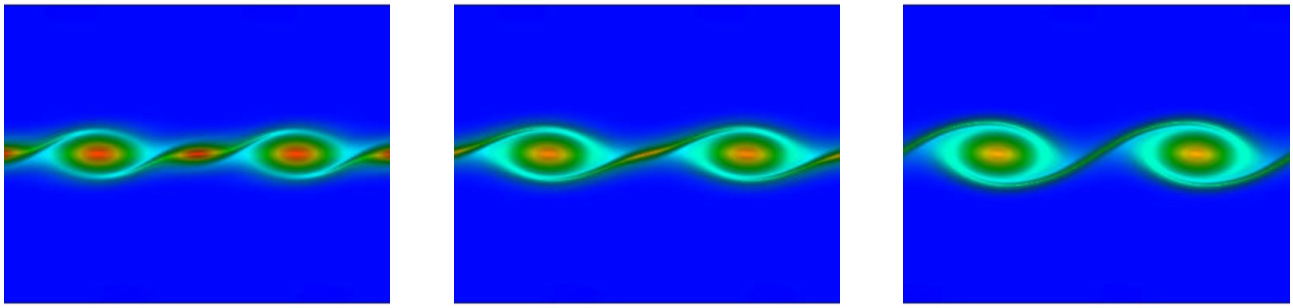

Figure 8: Nonlinear evolution of disturbance composed of a mode with wavenumber $\pi/8$ and another with wavenumber $3\pi/16$, in double precision accuracy. The frames presented correspond to the nondimensional times 96, 115.2 and 124.8.

7. References

Betchov, R. and Criminale, W. O., 1967, "Stability of parallel flow", Academic press.

Fortuné, V., 2000, "Étude par Simulation Numérique Directe du rayonnement acoustique de couches de mélabge isothermes et anisothermes", PhD thesis, Université de Poitier.

Herbert, T., 1988, Secondary instability of boundary layers, "Ann. Rev. Fluid Mech.", Vol. 20, pp. 487–526.

Lele, S., 1992, Compact Finite Difference Schemes with Spectral-like Resolution, "J. Computational Physics", Vol. **103**, pp. 16–42.

Medeiros, M. A. F., 2000, nonlinear hydrodynamic instability, "II school of transition and turbulence", pp. 312–357, Uberlândia – Brazil. in portuguese.

Mendonça, M. T., 2000, Laminar flow stability: linear theory, "II school of transition and turbulence", pp. 98–147, Uberlândia – Brazil.

Michalke, A., 1964, SOn the inviscid instability of the hyperbolic-tangent velocity profile, "J. Fluid Mech.", Vol. 19, pp. 543–566.

Sandham, N. D. and Reynolds, W. C., 1991, TThree-dimensional simulations of large eddies in the compressible mixing layer, "J. Fluid Mech.", Vol. 224, pp. 133–158.

Silvestrini, J. H., 2000, Direct Numerical Simulation and Large Eddy Simulation of Transitional and Turbulent Flows, "II school of transition and turbulence", pp. 148–219, Uberlândia – Brazil. in portuguese.

Tatsumi, T. and Gotoh, K., 1960, The stability of free boundary layers between two uniform streams, "J. Fluid Mech.", Vol. 7, pp. 433–441.

von Terzi, D. A., Linnick, M. N., Seidel, J., and Fasel, H., 2001, Immersed boundayr techniques for high-order finite -difference methods, "31th AIAA Fluid Dynamics Conference", pp. 1–17, Anaheim, CA.

Williamson, J. H., 1980, Low-storage Runge-Kutta Schemes, "J. Comp. Phys.", Vol. 35, pp. 48–56.